Optogenetically induced sleep spindle rhythms alter sleep architectures in mice

Angela Kim[a,b,c], Charles Latchoumane[a], Soojung Lee[d,e], Guk Bae Kim[b], Eunji Cheong[f], George J. Augustine[d,g], and Hee-Sup Shin[a,c,1]

[a]Center for Cognition and Sociality, Institute for Basic Science, Yusung-gu, Daejeon 305-811, Korea; [b]Center for Neuroscience, Brain Science Institute, Korea Institute of Science and Technology, Hwarangno, Seoul 136-791, Korea; [c]Department of Neuroscience, University of Science and Technology, Daejeon 305-350, Korea; [d]Center for Functional Connectomics, Brain Science Institute, Korea Institute of Science and Technology, Seoul 136-791, Korea; [e]Department of Maxillofacial Tissue Regeneration, School of Dentistry, Kyung Hee University, Seoul 130-701, Korea; [f]Department of Biotechnology, Translational Research Center for Protein Function Control, College of Life Science and Biotechnology, Yonsei University, Seoul 120-749, Korea; and [g]Program in Neuroscience and Behavioral Disorder, Duke-NUS Graduate Medical School, Singapore 169857

Contributed by Hee-Sup Shin, October 25, 2012 (sent for review September 13, 2012)

Sleep spindles are rhythmic patterns of neuronal activity generated within the thalamocortical circuit. Although spindles have been hypothesized to protect sleep by reducing the influence of external stimuli, it remains to be confirmed experimentally whether there is a direct relationship between sleep spindles and the stability of sleep. We have addressed this issue by using in vivo photostimulation of the thalamic reticular nucleus of mice to generate spindle oscillations that are structurally and functionally similar to spontaneous sleep spindles. Such optogenetic generation of sleep spindles increased the duration of non-rapid eye movement (NREM) sleep. Furthermore, the density of sleep spindles was correlated with the amount of NREM sleep. These findings establish a causal relationship between sleep spindles and the stability of NREM sleep, strongly supporting a role for the thalamocortical circuit in sleep regulation.

sleep rhythms | sleep protection

Sleep spindles are characteristic EEG rhythms observed during non-rapid eye movement (NREM) sleep. It is characterized by periodic waxing and waning and 7- to 15-Hz oscillations with durations ranging from 0.5 to 3 s (1–3), and is often used as an EEG marker of NREM sleep. Sleep spindles are hypothesized to originate from the thalamic reticular nucleus (TRN) (4, 5), where the rhythmic burst activity of TRN neurons could initiate spindle oscillations within the whole thalamocortical circuit. When it has been initiated, this oscillation is self-maintained by the reciprocal interactions among cortical, thalamocortical (TC), and TRN neurons during NREM sleep (4, 6, 7). Sleep spindles are of particular interest because they are known to be involved in several sleep-dependent physiological and cognitive processes, such as memory consolidation and neuronal plasticity (7–10). Moreover, a growing amount of evidence suggests that sleep spindles serve a sleep-protecting function by modulating the degree of sensory transmission through the thalamus (11). Patients with hypersomnia show increased spindle density (SD) compared with control (12), and KO mice whose sleep spindles are reduced as a result of impaired thalamocortical oscillations experience sleep disturbances during NREM sleep (13–16). Further, individuals with a higher spindle rate are more tolerant to noise that occurs during sleep (17). Despite considerable evidence hinting at the sleep-protecting function of sleep spindles, no experimental studies have yet demonstrated a direct causal relationship between sleep spindles and the stability of sleep. A recent study found that optogenetic stimulation of TRN induced burst firing in TC neurons, which were hypothesized to underlie the occurrence of neocortical sleep spindles (18). However, because sleep spindles also occur spontaneously, it was not clear whether sleep spindles were driven by optogenetic stimulation of the TRN.

To experimentally examine the sleep-protecting function of sleep spindles, we used Channelrhodopsin2 (ChR2) transgenic (tg) mice to bilaterally modulate the TRN with photostimulation protocols that mimic the EEG rhythms of sleep spindles. We found that neocortical sleep spindles are readily induced in vivo by optogenetic stimulation of TRN at a spindle-like frequency, and such stimulation increased the total duration of NREM sleep. Thus, the number of sleep spindles is correlated with the amount of NREM sleep. These results reveal the critical role that thalamocortical circuits play in the regulation of sleep and strongly support the idea that sleep spindles protect NREM sleep.

Results

Photostimulation of Thalamic Reticular Neurons. We started by examining our ability to use light to control the activity of ChR2-expressing neurons in slices prepared from the TRN of Thy1-ChR2 mice (19). These neurons were identified by the location of their cell bodies (Fig. 1*A*) within the TRN region and by their responses to injected currents. TRN neurons could be identified because they showed no time-dependent depolarization in response to hyperpolarizing currents (Fig. 1*B*), unlike other thalamic neurons that exhibit such responses as a result of hyperpolarization-activated currents (20). Many TRN neurons displayed rhythmic, high-frequency bursts of action potentials (APs) followed by stretch of tonic firings in response to depolarizing currents, as observed for the neuron shown in Fig. 1*B*. However, this was not always observed, as reported previously (21, 22).

Illumination evoked photocurrents in ChR2-positive TRN neurons (Fig. 1*C*). These currents activated rapidly and partially inactivated during prolonged illumination. To generate different patterns of AP firing, we photostimulated these neurons with three different protocols. To simulate the rhythmic spike-bursts observed during sleep spindles, we photostimulated TRN neurons with brief light pulses (62 ms duration) at 8 Hz, the intrinsic frequency of sleep spindles (i.e., spindle-like protocol) (4, 23). Such stimuli were repeated at intervals of 7.5 s, the average interval between sleep spindles (2, 4). A second stimulus protocol consisted of 200-ms-duration light flashes repeated at 1 Hz (i.e., 1-Hz protocol); these were intended to mimic slow wave responses during NREM sleep (23–25). Finally, we used a third photostimulation protocol consisting of 20-ms-duration stimuli repeated at 0.1 Hz that has been previously reported to produce thalamic bursts and cortical spindles in vivo (i.e., pulse protocol) (18).

Representative examples of AP responses to these three photostimulation protocols are shown in Fig. 1*D*. Spindle-like stimulation reliably generated repetitive burst firing activity during photostimulation, whereas 1-Hz stimulation resulted in

Author contributions: A.K., C.L., G.B.K., E.C., G.J.A., and H.-S.S. designed research; A.K. and S.L. performed research; A.K., C.L., and S.L. analyzed data; and A.K., G.J.A., and H.-S.S. wrote the paper.

The authors declare no conflict of interest.

[1]To whom correspondence should be addressed. E-mail: shin@ibs.re.kr.

This article contains supporting information online at www.pnas.org/lookup/suppl/doi:10.1073/pnas.1217897109/-/DCSupplemental.

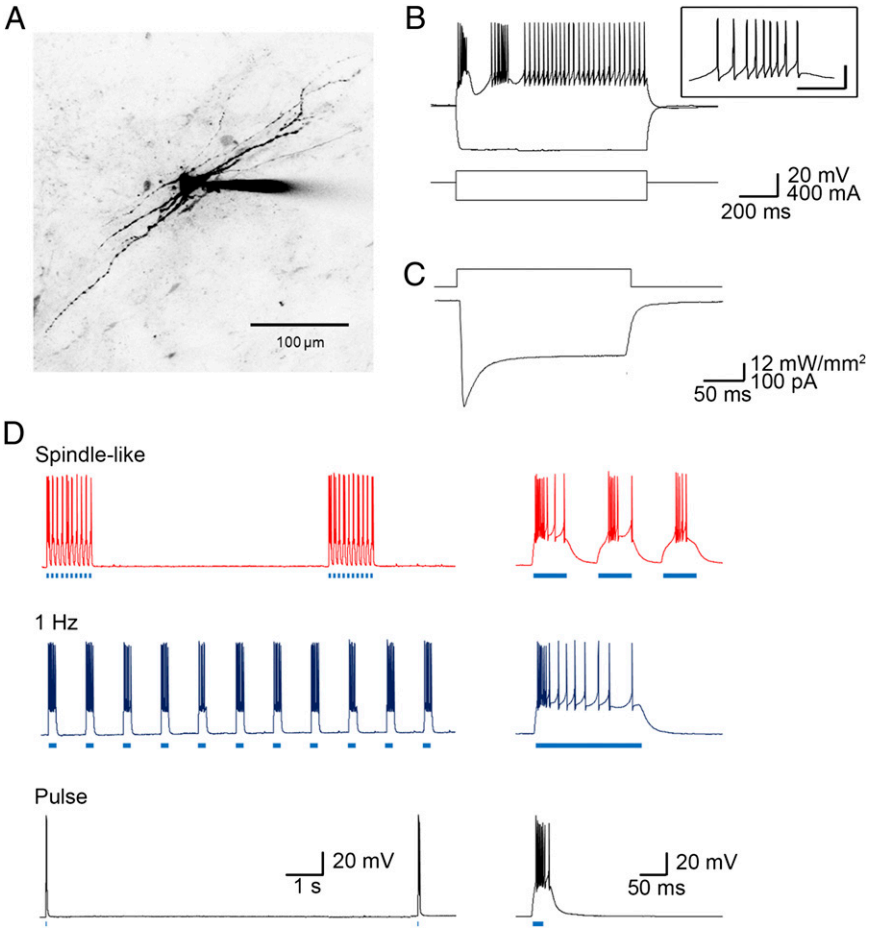

Fig. 1. Characterization of TRN neuron firing in response to photostimulation with three different protocols. (*A*) *Left*: Structure of TRN neuron, visualized by the fluorescent dye lucifer yellow. For clarity, image contrast was inverted so that fluorescence is shown as black. (*B*) Changes in membrane potential (*Upper*) evoked by current pulses (*Lower*). *Inset*: Characteristic accelerando-decelerando pattern of bursts in TRN neurons. (Scale bar: *Inset*, 20 mV, 50 ms.) (*C*) Photocurrent (*Lower*) elicited by illumination (*Upper*) of a ChR2-expressing TRN neuron. Holding potential was −60 mV. Photocurrent was pharmacologically isolated from synaptic responses by treatment of the slice with 10 μM CNQX, 50 μM AP-5, and 20 μM bicuculline. (*D*) Examples of AP responses induced in a TRN neuron in response to the three different photostimulation protocols. Light flashes are indicated by blue bars. Responses to the first photostimulation of each protocol are enlarged on the right.

high-frequency bursts followed by gradual loss of spiking and eventually spike failure over the course of several minutes of stimulation. In both cases, initial high-frequency bursts were often followed by tonic spikes that extended toward the end of each stimulation pulse. The pulse photostimulation protocol induced spike bursts, occasionally followed by rhythmic bursts. In summary, although all three stimulus protocols elicited bursts of APs, the interburst structure differed in each case.

Efficient Induction of EEG Sleep Spindle Rhythms by Photostimulation of TRN. We next applied the same photostimulation protocols to the TRN region in vivo to identify the stimulus that most effectively induced neocortical EEG sleep spindles (Fig. S1). We performed 1-h EEG recordings from freely moving mice during daytime, the inactive period for mice, with each stimulation protocol applied throughout the recording session. The pulse protocol was applied to the TRN unilaterally or bilaterally to ensure that our procedures match those previously used (18). Spindle-like or 1-Hz stimuli were applied bilaterally.

Average EEG power spectrograms showed that photostimulation of TRN induced clear responses by increasing the power within specific frequency ranges (Fig. 2*A*). The spindle-like photostimulation protocol caused a pronounced increase in power that was maximal at 8 Hz, the photostimulus frequency. This increase was sustained throughout the duration of photostimulation. The 1-Hz and bilateral pulse protocols also evoked strong responses in the EEG. There were, however, important differences compared with the responses evoked by the spindle-like protocol. The affected frequency range was lower (4–5 Hz) than that of the spindle-like protocol, and the response was briefer, never exceeding 0.5 s. The unilateral pulse protocol did not cause any distinguishable changes in EEG power.

Next, we compared the efficiency of each photostimulation protocol in increasing power specifically at the sleep spindle frequency (7–15 Hz). The spindle-like protocol caused the greatest increase in spindle power, with the response remaining nearly constant throughout the 1.25 s of photostimulation (Fig. 2*B*). The 1-Hz protocol also induced a similar increase in spindle power, but the increase lasted only for a brief period. The response to the bilateral pulse protocol was weaker than that produced by the 1-Hz protocol. The unilateral pulse protocol did not induce any observable changes in the spindle power.

Next, we examined the raw EEG traces to investigate whether photostimulation of TRN could induce neocortical sleep spindles. Visual inspection of raw EEG traces clearly revealed distinct patterns of evoked EEG responses for each protocol (Fig. 2 *C* and *D*). EEG responses evoked by the spindle-like photostimulation protocol were characterized by large-amplitude phasic oscillations that met the conventional criteria used to define sleep spindles (1–3). Most of these evoked responses were temporally separate from spontaneous sleep spindles, and photostimulation did not disturb the natural progression of spontaneous sleep spindles. Unlike the spindle-like protocol, the 1-Hz photostimulation protocol did not seem to initiate sleep spindles. Instead, EEG responses evoked by 1-Hz stimulation were distinguished by the presence of a single large-amplitude peak at the beginning of the 200-ms photostimulus (Fig. 2*D*, *Right*). Spontaneous sleep spindles were observed throughout the NREM period and did not appear to have any temporal relationship with the 1-Hz stimulus pulses. EEG responses to the unilateral or bilateral pulse stimuli were similar to those to the 1-Hz photostimulation and consisted of brief single

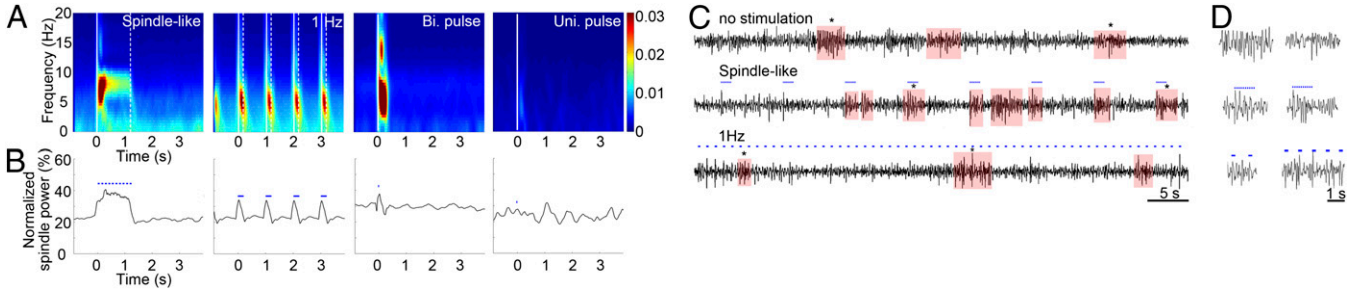

Fig. 2. Spindle-like photostimulation on TRN induces neocortical sleep spindles. (*A*) Average peristimulus power spectrograms of EEG following spindle-like, 1-Hz, and bilateral and unilateral pulse photostimulation at time 0. White solid and dotted lines indicate start and end of the photostimulation pulses, respectively. Shown is an average from one recording ($n = 356$ stimulations from each photostimulation protocol). (*B*) Changes in relative spindle power (7–15 Hz) following photostimulation with spindle-like, 1-Hz, and bilateral and unilateral pulse photostimulation at time 0. Photostimulation pulses are indicated by blue bars. Shown is an average from one recording ($n = 356$ stimulations from each photostimulation protocol). (*C*) Representative traces of 1-min EEG recording during NREM sleep showing spontaneous and evoked spindles (gray boxes) for no stimulation, spindle-like, and 1-Hz stimulation protocols. Light pulses are indicated by blue bars. Shown is an example from one mouse. (*D*) Two examples of sleep spindles during no stimulation (*Top*), spindle-like (*Middle*), and 1-Hz stimulation (*Bottom*) protocols. Sleep spindles marked with asterisks in *A* are enlarged to show the waveforms. Light pulses are indicated by blue bars. Spindle-like photostimulation evoked sleep spindles with waveforms nearly identical to the spontaneous sleep spindles observed without stimulation.

peaks of large amplitude (Fig. S2 *A* and *B*). These were not sleep spindles because their duration was too brief to meet the criteria for sleep spindles (1–3).

We next examined the power spectra of sleep spindles detected during each of the photostimulation protocols. Sleep spindles occurring during the spindle-like protocol were highly regular at 8 Hz, the same frequency as the photostimuli, and showed a second harmonic around 16 Hz ($n = 30$ recordings per condition; Fig. S2*E*). The high power at 8 Hz was also clearly visible when the total NREM power was considered (Fig. S2*D*), and such response to the spindle-like photostimulation remained consistent throughout NREM sleep (Fig. S2*D*). In contrast, the power spectrum of sleep spindles detected during the 1-Hz protocol had reduced power within the spindle frequency range, whereas the power at higher frequencies (>15 Hz) was significantly increased compared with that of spontaneous sleep spindles (Fig. S2*E*). No significant differences were found between the power profiles of the spontaneous sleep spindles and those in occurring during the uni- and bilateral pulse protocols.

Together, these results show that the spindle-like photostimulation protocol could selectively induce sleep spindles that are structurally similar to the spontaneous spindles, whereas the responses evoked by the 1-Hz or uni- or bilateral pulse protocols were usually too brief to be considered as sleep spindles.

Increased Sleep SD During Spindle-Like Photostimulation of TRN. As a different way to compare the ability of the different photostimulation protocols to evoke sleep spindles, we determined the probability that a sleep spindle was produced in response to each photostimulus. The rate of co-occurrence of spindles was highest for spindle-like photostimulation ($n = 30$ recordings, $n = 5$ recordings per condition per mouse, $n = 6$ mice; Fig. 3*A* and Table S1). Sleep spindles coincided with 51.1 ± 2.6% of the total number of spindle-like photostimuli whereas the values for the 1-Hz and uni- or bilateral pulse photostimulation protocols were significantly lower (3.2 ± 0.8%, 3.6 ± 7.1%, and 0%, respectively; mean ± SEM). This suggests that only the spindle-like photostimulation protocol was capable of evoking EEG sleep spindles.

Next, to determine whether the sleep status of the mouse affected our ability to induce sleep spindles via photostimulation, we compared spindle co-occurrence rates during wake and NREM sleep states. Spindle co-occurrence rates were higher during NREM sleep than during wake states for 1-Hz and uni- and bilateral pulse photostimulation (Fig. 3*A* and Table S1). This probably reflects the higher propensity of the thalamocortical circuit to generate sleep spindles during NREM sleep. In contrast, during the spindle-like protocol, co-occurrence rates were lower during NREM sleep than during the wake state (Fig. 3*A*). This indicates that this protocol effectively induced sleep spindles even during the wake state, when the thalamocortical circuit is less able to generate spontaneous sleep spindles. The lower spindle co-occurrence rate during NREM sleep, compared with the wake state, might be caused by the high rate of spontaneous sleep spindles during NREM limiting further optogenetic induction of sleep spindles.

Next, we quantified the density of EEG sleep spindles (i.e., SD) produced by the four protocols. SDs were calculated

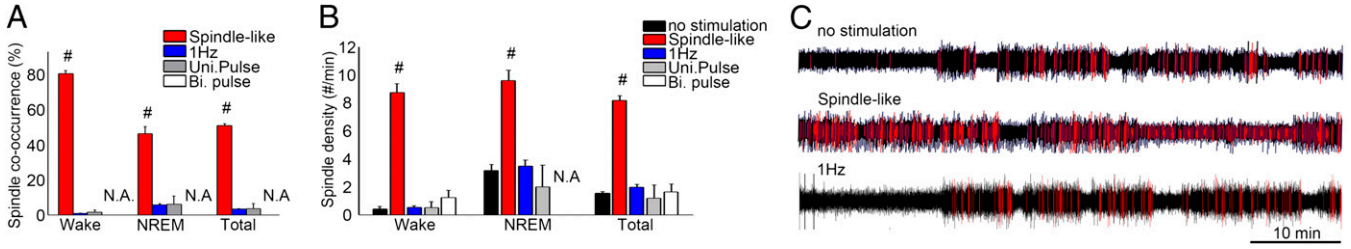

Fig. 3. Spindle-like photostimulation protocol is most effective in inducing neocortical sleep spindles. (*A*) Average spindle co-occurrence rates during wake, NREM, and total recording periods for spindle-like, 1-Hz, and uni- and bilateral pulse protocols. Numbers are the same as in Table S1. Data represent the mean ± SEM ($n = 6$ mice; $n = 5$ recordings per condition per mouse; $^{\#}P < 0.01$, nonparametric Wilcoxon rank-sum test). (*B*) Average spindle densities during wake, NREM, and total recording periods for spindle-like, 1-Hz, and uni- and bilateral pulse protocols. Numbers are the same as in Table S2. Data represent the mean ± SEM ($n = 6$ mice; $n = 5$ recordings per condition per mouse; $^{\#}P < 0.01$, nonparametric Wilcoxon rank-sum test). (*C*) Representative traces of 1-h EEG recording showing distribution of sleep spindles (red) for no stimulation, spindle-like, and 1-Hz stimulation protocols. Shown is an example from one mouse.

separately for wake, NREM, and REM states, and these values were averaged to give SDs for the total duration of the recording. The spindle-like protocol gave the highest SDs, whether for the overall duration of the recording, during the wake state, or during NREM sleep (n = 30 recordings, n = 5 recordings per condition per mouse, n = 6 mice; Fig. 3*B* and Table S2). These values were significantly higher than the SDs of spontaneous spindles ($P < 0.01$, nonparametric Wilcoxon rank-sum test). In contrast, 1-Hz and uni- and bilateral pulse photostimuli did not cause significant changes in SD during any of the states ($P > 0.05$). The effect of spindle-like photostimulation on SD was apparent when representative 1-h EEG traces from each protocol were compared (Fig. 3*C*). Spindle-like photostimulation of the TRN effectively increased the occurrence of sleep spindles during wake and NREM sleep states (Table S1). Spindle-like protocols with different frequencies (10 and 12 Hz) were ineffective in increasing the SD (Fig. S2*C*). This demonstrates that the effect of this protocol was not caused by any nonspecific effect of illumination such as local heating of TRN.

Sleep analysis revealed that the bilateral pulse photostimulation protocol was inappropriate for our study. When this protocol was applied, sleep (NREM and REM sleep) was almost absent in two of six mice during the continuous 3-h recordings, suggesting that it disturbs the normal sleep behavior of mice. Therefore, we did not use the pulse protocol in subsequent behavioral experiments.

Spindle-Like Photostimulation Increases NREM Sleep at the Expense of Wake State. Next, we examined the effect of spindle-like photostimulation on the sleep–wake architecture of mice during daytime. We found that spindle-like photostimulation significantly increased the total duration of NREM sleep ($P < 0.05$, nonparametric Wilcoxon rank-sum test; n = 6 mice per condition; Fig. 4*A*), whereas time spent awake decreased significantly compared with unstimulated controls ($P < 0.05$). The number of transitions between NREM and REM [both NREM-to-REM (NR) and REM-to-NREM (RN)] were also significantly increased ($P < 0.05$, nonparametric Wilcoxon rank-sum test; Fig. 4 *B* and *D*), but no significant changes ($P > 0.05$) were found in any other transitions between the sleep states [wake-to-NREM (WN), NREM-to-wake (NW), REM-to-wake (RW)]. On the contrary, photostimulation with the 1-Hz protocol, which did not induce significant changes in SD during any state ($P > 0.05$; Fig. 3*B*), did not cause any significant changes in the total duration of sleep or wake states ($P > 0.05$; Fig. 4*A*).

Next, to determine whether the spindle-like photostimulation altered the duration of individual wake episodes, we compared the cumulative distributions of the duration of single wake episodes (Fig. 4*C*). We found a significant difference in the distributions between the spindle-like protocol and the no stimulation group ($P < 0.001$, two-sample Kolmogorov–Smirnov test on pooled data of six mice). On the contrary, no significant difference was found between the distributions for the 1-Hz protocol and the no-stimulation group ($P = 0.2$). In the distribution of the spindle-like protocol, a clear reduction in the occurrence of wake episodes with long durations (>20 min) was apparent, as indicated by a gradual decrease in slope of the distribution curve after 20 min compared with the no-stimulation case. Moreover, the values for the spindle-like protocol remained constant in the later part of the graph, with a complete absence of wake episodes exceeding 35 min. On the contrary, there were no significant changes in the durations of individual NREM or REM episodes ($P > 0.05$; Fig. S3*A*). These results suggest that spindle-like photostimulation increases the total duration of NREM sleep at the expense of wake state.

Previous studies have suggested a positive relationship between SD and the duration or stability of sleep, with sleep spindles regulating transitions between NREM and REM sleep states (2, 12, 17). To establish whether the increase in SD is quantitatively related to the changes in NREM sleep duration or in the number of sleep state transitions, we examined the correlation between these values. We found a significant positive correlation between SD and the duration of NREM sleep ($R = 0.5987$; $P < 0.01$, Pearson correlation coupled to a least-square regression method with 95% CI; n = 6 mice per condition; Fig. 5*A*).

To study the relationship between SD and the sleep state transitions, we next examined the relationship between the average SD during the 1 min immediately preceding each NR transition ($SD_{pre\text{-}REM}$) and the total number of NR transitions. Across all three photostimulation protocols, we found a significant positive correlation between $SD_{pre\text{-}REM}$ and the number of NR transitions ($R = 0.5468$; $P = 0.0189$, Pearson correlation coupled to a least-square regression method with 95% CI; n = 6 mice per condition; Fig. 4*C*). Additionally, we analyzed instantaneous SDs during the 1 min before each NR transition to compare the dynamics of SD before NR transition during each photostimulation protocols (Fig. S3*B*). We found an abrupt increase in SD before the NR transition for all three cases, a result consistent with previous reports (2, 26). Throughout the 1-min period, the SD remained the highest for the spindle-like case. This suggests that spindle-like photostimulation modulates the number of NR transitions. These results confirm that an

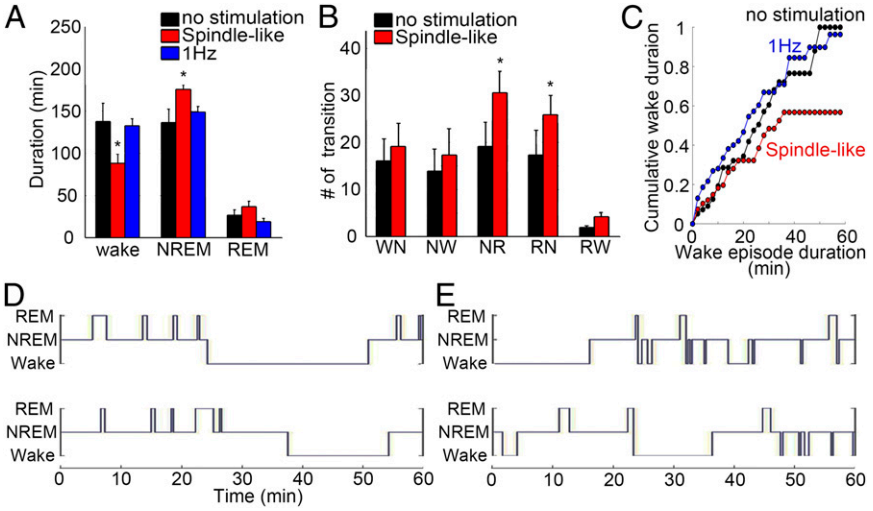

Fig. 4. Spindle-like photostimulation on TRN alters sleep–wake architecture. (*A*) Total duration spent awake, in NREM, and in REM during spindle-like and 1-Hz photostimulation. Data represent the mean ± SEM (n = 6 mice, n = 5 recordings per condition per mouse; *$P < 0.05$, nonparametric Wilcoxon rank-sum test). (*B*) Total number of sleep state transitions during 5 h of photostimulation with spindle-like protocol. Data represent the mean ± SEM (n = 6 mice, n = 5 recordings per condition per mouse; *$P < 0.05$, nonparametric Wilcoxon rank-sum test). (*C*) Cumulative distribution of single wake episodes during no stimulation, spindle-like stimulation, and 1-Hz photostimulation. Values are normalized to the final cumulative value of the no-stimulation case. Data represent the mean ± SEM (n = 6 mice, n = 5 recordings per condition per mouse; two-sample Kolmogorov–Smirnov test on pooled data of six mice). (*D* and *E*) Representative hypnograms during spindle-like (*D*) and 1-Hz (*E*) photostimulation.

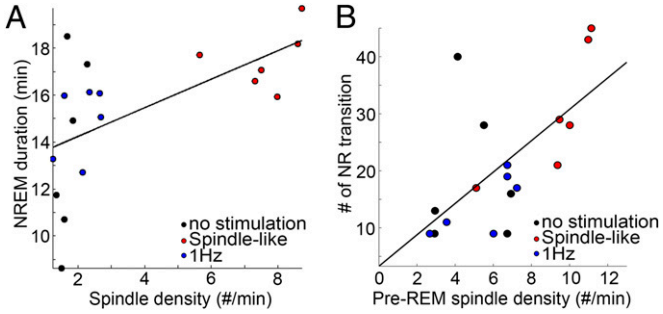

Fig. 5. Sleep SD positively correlates with the NREM sleep duration. (*A*) Correlation analysis between average spindle densities during whole recording period and the total NREM sleep duration. Each point represents the average data from one mouse ($n = 6$ mice, $n = 5$ recordings per condition per mouse; $^{*}P < 0.05$, $^{\#}P < 0.01$, Pearson correlation coupled to least-square regression method with 95% CI). (*B*) Correlation analysis between average $SD_{pre\text{-}REM}$ and number of NR transitions during spindle-like photostimulation. Each point represents the average data from one mouse ($n = 6$ mice, $n = 5$ recordings per mouse; Pearson correlation coupled to least-square regression method with 95% CI).

increase in SD is quantitatively related to and directly responsible for the changes in sleep–wake architecture observed during the spindle-like photostimulation. It also suggests that optogenetically induced sleep spindles are functionally similar to the spontaneous sleep spindles in regard to their relationship to the duration of NREM sleep and sleep state transitions.

Discussion

Our study demonstrates that neocortical sleep spindles can be induced reliably in vivo by optogenetic stimulation of TRN. We also provide direct evidence for a causal relationship between sleep spindles and the stability of sleep. We established a photostimulation protocol that effectively induces sleep spindles that are functionally and structurally similar to the spontaneous sleep spindles. Increasing SD with this protocol increased the total duration of NREM sleep, proving the longstanding hypothesis that sleep spindles protect sleep.

Sleep-Protecting Function of Sleep Spindles. The thalamus is a sensory relay station that gates the flow of peripheral sensory information to the cortex (27–29). TC neurons, the major relay neurons of the thalamus, have strong reciprocal connections with GABAergic TRN neurons, and synaptic interactions between them can generate sustained network oscillations, such as sleep spindles. Sleep spindle rhythms have long been thought to protect sleep; TC neurons are able to generate APs in two distinct modes—tonic and burst—in response to changes in their membrane potential. The repetitive postinhibitory rebound burst firing that occurs in TC neurons following increased inhibitory inputs from the TRN and underlies neocortical sleep spindles is hypothesized to hinder the reliable transmission of external stimuli to the cortex (30), thereby increasing the tolerance to noise during sleep.

The sleep-protecting function of sleep spindles is supported by a number of EEG and neuroimaging studies in humans; for example, brain responses to auditory stimulus are significantly reduced when a tone is delivered concurrently with sleep spindles (31). Other studies have demonstrated a positive correlation between SD and the duration or stability of sleep (12, 17), suggesting that the amount of sleep spindles might signify the strength of the gatekeeping mechanism that the thalamus exerts during sleep. However, these studies cannot establish a causal role for sleep spindles in regulating sleep behavior because it was not possible to directly control SD while preserving normal functioning of the brain. Our study demonstrates that SD can be modulated in vivo by optogenetic control of TRN. Our results provide experimental evidence for the sleep-protecting function of sleep spindles by showing that artificially increasing SD by optogenetic stimulation results in an increase in the total duration of NREM sleep.

It is known that EEG σ-power (10–14 Hz) and SD abruptly increases at the pre-REM period (2). The spindles occurring during this phase (pre-REM spindles) are larger in amplitude and longer in duration than the sleep spindles observed during other phases of NREM sleep (32). This is consistent with the observation that TRN neurons fire maximally during the pre-REM period (33). Pre-REM spindles have been suggested to control the initiation of REM sleep, as normal NR transitions invariably are preceded by pre-REM spindles. Further, in orexin KO mice, narcoleptic attacks, which are abnormal transitions from wake to REM sleep, are linked to the brief occurrence of an EEG signal that resembles pre-REM EEG activity (34). Indeed, we observed similar pre-REM EEG activity before NR transitions in our recordings. Our results indicate that the increase in the total duration of NREM sleep is caused by an increase in the number of NR and RN transitions and a reduced number of long wake episodes (>20 min), whereas the average duration of NREM or REM sleep episodes was unaffected. Moreover, the $SD_{pre\text{-}REM}$ positively correlated with the number of NR transitions, and we observed an additional increase in pre-REM spindles during spindle-like photostimulation.

Therefore, we conclude that sleep spindles might protect sleep by increasing sleep stability by blocking the transmission of external sensory stimuli, as well as by facilitating the transition from NREM sleep to REM sleep. These dual sleep-protecting functions might depend on the temporal location of sleep spindles during NREM sleep.

Efficiency of Optogenetic Induction of Neocortical Sleep Rhythms. Our current knowledge of the neurophysiological mechanisms underlying sleep spindles largely depends on in vitro studies. The unique ability of TRN neurons to fire in rhythmic spike-bursts in response to decreased inhibitory inputs from wake-promoting cell groups in the brainstem results in a subsequent alteration in the activity of TC and cortical neurons, leading to the generation of sleep spindles during NREM sleep (4, 35). However, this hypothesis awaits further validation in vivo in behaving mice.

By using optogenetic techniques in vivo, we demonstrated that spindle-like photostimulation of TRN was sufficient to induce neocortical sleep spindles in behaving mice. Moreover, in vitro recordings from TRN neurons showed that spindle-like photostimuli could reliably evoke repetitive burst firing activity, which is comparable to the rhythmic spike-burst activity of TRN neurons (5, 23, 24). This is an intrinsic firing pattern of TRN neurons during NREM sleep and is hypothesized to be the main factor that drives generation of sleep spindles (4, 23). Further experiments using these photostimulation protocols on defined neuronal populations within the thalamocortical circuit may reveal the full cellular and circuit mechanisms underlying diverse sleep-related rhythms in these brain regions.

We proved that our spindle-like protocol is a robust tool to induce sleep spindles in behaving mice. A total of 51.12 ± 2.63% of the spindle-like stimulations coincided with the occurrence of EEG sleep spindles conforming to conventional criteria, and the efficiency of spindle induction was not affected by the vigilance states of the mice. In contrast, inconsistent with a previous report (18), we could not induce sleep spindles by using the pulse stimulation protocol. In fact, the previous report also did not provide clear evidence of optogenetic induction of sleep spindles: although optogenetic stimulation of TRN induced burst firing in TC neurons, which is hypothesized to underlie sleep spindles (18), the responses shown do not meet the conventional criteria for sleep

spindles as a result of their short duration. Moreover, the fact that responses were largely limited to the NREM sleep period raises the possibility that sleep spindles occurred spontaneously rather than as a result of optogenetic stimulation. Thus, it remains to be determined whether there are conditions in which the pulse stimulation protocol can generate sleep spindles.

In our results, although the peristimulus power spectral analysis showed an abrupt increase in the spindle frequency power immediately following the pulse photostimulation, the effect was too short to be defined as a sleep spindle according to our conventional criteria (1–3). Average SD also showed no significant changes after the pulse photostimulation. Indeed, the repetitive rhythmic spike-burst activity of TRN neurons, which is the neuronal basis for neocortical sleep spindle, usually lasts for several seconds (5, 6, 36). This explains why the 20-ms pulse photostimulation failed to generate sleep spindles in our study whereas the spindle-like photostimulation was very effective. Single spikes in TRN neurons, triggered by pulse photostimulation, might be insufficient to trigger an oscillatory event in the entire thalamocortical circuit. Performing similar photostimulation experiments on specific Ca^{2+} channel KO mice showing impaired rhythmic spike-burst activity in TRN neurons, e.g., R- or T-type Ca^{2+} channel KO mice, will help elucidate the role of rhythmic activity of TRN neurons in generating sleep spindles.

The 1-Hz photostimulation protocol was ineffective in triggering neocortical slow waves. Slow-wave oscillations differ from sleep spindles in being of cortical origin. Intrinsically oscillating intracortical networks involving glutamatergic pyramidal neurons and GABAergic local interneurons are thought to be responsible for the occurrence and spread of slow wave oscillation throughout the cortex (4, 37). Slow waves can be observed in the cortex after extensive thalamic lesion, emphasizing minimal contribution of TC and TRN neurons to this sleep rhythm (38). Therefore, despite the efficiency of 1-Hz photostimulation in inducing activity of TRN neurons that is comparable to what is observed during natural slow-wave sleep (28–30), this apparently is insufficient to recruit the self-oscillating neocortical networks needed to initiate full-blown slow wave oscillation.

Our findings indicate an essential role for sleep spindles in sleep regulation and suggest that the thalamocortical circuit is a critical part of the sleep-regulatory network. These results provide a valuable insight into the thalamocortical circuit as a therapeutic and diagnostic target for the treatment of sleep-related neurological illnesses. Moreover, our results show that modulation of sleep spindles may prove to be an effective treatment for restoring normal sleep architecture in patients with disrupted sleep. In addition, our optogenetic protocol for sleep spindle generation in behaving mice will allow full exploration of the functions of this brain oscillation in sleep-related physiological and cognitive processes.

Materials and Methods

ChR2 tg mice were purchased from the Jackson Laboratories [B6.Cg-Tg (Thy1::COP4/EYFP)18Gfng/J] (19). Sleep recordings were conducted by using male heterozygote mice. Animal care and all experiments were conducted in accordance with the ethical guidelines of the Institutional Animal Care and Use Committee of the Korea Institute of Science and Technology. Detailed descriptions of study methods are provided in *SI Materials and Methods*.

ACKNOWLEDGMENTS. This work was supported by grants from Institute for Basic Science, the National Honor Scientist Program of Korea, and the World Class Institute (WCI) Program of the National Research Foundation of Korea (NRF) (WCI 2009-003) funded by the Ministry of Education, Science and Technology of Korea (MEST) and by a Competitive Research Program grant from the National Research Foundation of Singapore.

1. De Gennaro L, Ferrara M (2003) Sleep spindles: An overview. *Sleep Med Rev* 7(5):423–440.
2. Vyazovskiy VV, Achermann P, Borbély AA, Tobler I (2004) The dynamics of spindles and EEG slow-wave activity in NREM sleep in mice. *Arch Ital Biol* 142(4):511–523.
3. Dijk DJ (1995) EEG slow waves and sleep spindles: Windows on the sleeping brain. *Behav Brain Res* 69(1-2):109–116.
4. Steriade M, McCormick DA, Sejnowski TJ (1993) Thalamocortical oscillations in the sleeping and aroused brain. *Science* 262(5134):679–685.
5. Steriade M, Domich L, Oakson G, Deschênes M (1987) The deafferented reticular thalamic nucleus generates spindle rhythmicity. *J Neurophysiol* 57(1):260–273.
6. von Krosigk M, Bal T, McCormick DA (1993) Cellular mechanisms of a synchronized oscillation in the thalamus. *Science* 261(5119):361–364.
7. Llinás RR, Steriade M (2006) Bursting of thalamic neurons and states of vigilance. *J Neurophysiol* 95(6):3297–3308.
8. Stickgold R (2005) Sleep-dependent memory consolidation. *Nature* 437(7063): 1272–1278.
9. Steriade M, Timofeev I (2003) Neuronal plasticity in thalamocortical networks during sleep and waking oscillations. *Neuron* 37(4):563–576.
10. Fogel SM, Smith CT (2011) The function of the sleep spindle: A physiological index of intelligence and a mechanism for sleep-dependent memory consolidation. *Neurosci Biobehav Rev* 35(5):1154–1165.
11. Elton M, et al. (1997) Event-related potentials to tones in the absence and presence of sleep spindles. *J Sleep Res* 6(2):78–83.
12. Bové A, Culebras A, Moore JT, Westlake RE (1994) Relationship between sleep spindles and hypersomnia. *Sleep* 17(5):449–455.
13. Lee J, Kim D, Shin HS (2004) Lack of delta waves and sleep disturbances during non-rapid eye movement sleep in mice lacking alpha1G-subunit of T-type calcium channels. *Proc Natl Acad Sci USA* 101(52):18195–18199.
14. Anderson MP, et al. (2005) Thalamic Cav3.1 T-type Ca2+ channel plays a crucial role in stabilizing sleep. *Proc Natl Acad Sci USA* 102(5):1743–1748.
15. Blethyn KL, Hughes SW, Tóth TI, Cope DW, Crunelli V (2006) Neuronal basis of the slow (<1 Hz) oscillation in neurons of the nucleus reticularis thalami in vitro. *J Neurosci* 26(9):2474–2486.
16. Cueni L, et al. (2008) T-type Ca2+ channels, SK2 channels and SERCAs gate sleep-related oscillations in thalamic dendrites. *Nat Neurosci* 11(6):683–692.
17. Dang-Vu TT, McKinney SM, Buxton OM, Solet JM, Ellenbogen JM (2010) Spontaneous brain rhythms predict sleep stability in the face of noise. *Curr Biol* 20(15):R626–R627.
18. Halassa MM, et al. (2011) Selective optical drive of thalamic reticular nucleus generates thalamic bursts and cortical spindles. *Nat Neurosci* 14(9):1118–1120.
19. Wang H, et al. (2007) High-speed mapping of synaptic connectivity using photostimulation in Channelrhodopsin-2 transgenic mice. *Proc Natl Acad Sci USA* 104(19):8143–8148.
20. Abbas SY, Ying SW, Goldstein PA (2006) Compartmental distribution of hyperpolarization-activated cyclic-nucleotide-gated channel 2 and hyperpolarization-activated cyclic-nucleotide-gated channel 4 in thalamic reticular and thalamocortical relay neurons. *Neuroscience* 141(4):1811–1825.
21. Contreras D, Curró Dossi R, Steriade M (1992) Bursting and tonic discharges in two classes of reticular thalamic neurons. *J Neurophysiol* 68(3):973–977.
22. Lee J, Shin HS (2007) T-type calcium channels and thalamocortical rhythms in sleep: A perspective from studies of T-type calcium channel knockout mice. *CNS Neurol Disord Drug Targets* 6(1):63–69.
23. Steriade M, Domich L, Oakson G (1986) Reticularis thalami neurons revisited: Activity changes during shifts in states of vigilance. *J Neurosci* 6(1):68–81.
24. Muñoz F, Fuentealba P (2012) Dynamics of action potential initiation in the GABAergic thalamic reticular nucleus in vivo. *PLoS ONE* 7(1):e30154.
25. Steriade M, Contreras D, Curró Dossi R, Nuñez A (1993) The slow (< 1 Hz) oscillation in reticular thalamic and thalamocortical neurons: scenario of sleep rhythm generation in interacting thalamic and neocortical networks. *J Neurosci* 13(8):3284–3299.
26. Astori S, et al. (2011) The Ca(V)3.3 calcium channel is the major sleep spindle pacemaker in thalamus. *Proc Natl Acad Sci USA* 108(33):13823–13828.
27. Sherman SM (2001) Tonic and burst firing: Dual modes of thalamocortical relay. *Trends Neurosci* 24(2):122–126.
28. Steriade M, Llinás RR (1988) The functional states of the thalamus and the associated neuronal interplay. *Physiol Rev* 68(3):649–742.
29. Poulet JF, Fernandez LM, Crochet S, Petersen CC (2012) Thalamic control of cortical states. *Nat Neurosci* 15(3):370–372.
30. Weyand TG, Boudreaux M, Guido W (2001) Burst and tonic response modes in thalamic neurons during sleep and wakefulness. *J Neurophysiol* 85(3):1107–1118.
31. Dang-Vu TT, et al. (2011) Interplay between spontaneous and induced brain activity during human non-rapid eye movement sleep. *Proc Natl Acad Sci USA* 108(37): 15438–15443.
32. Gottesmann C, Gandolfo G, Arnaud C, Gauthier P (1998) The intermediate stage and paradoxical sleep in the rat: Influence of three generations of hypnotics. *Eur J Neurosci* 10(2):409–414.
33. Marks GA, Roffwarg HP (1993) Spontaneous activity in the thalamic reticular nucleus during the sleep/wake cycle of the freely-moving rat. *Brain Res* 623(2):241–248.
34. Chemelli RM, et al. (1999) Narcolepsy in orexin knockout mice: Molecular genetics of sleep regulation. *Cell* 98(4):437–451.
35. Saper CB, Fuller PM, Pedersen NP, Lu J, Scammell TE (2010) Sleep state switching. *Neuron* 68(6):1023–1042.
36. Contreras D, Steriade M (1996) Spindle oscillation in cats: the role of corticothalamic feedback in a thalamically generated rhythm. *J Physiol* 490(pt 1):159–179.
37. Crunelli V, Lorincz ML, Errington AC, Hughes SW (2012) Activity of cortical and thalamic neurons during the slow (<1 Hz) rhythm in the mouse in vivo. *Pflugers Arch* 463(1):73–88.
38. Steriade M, Nunez A, Amzica F (1993) Intracellular analysis of relations between the slow (< 1 Hz) neocortical oscillation and other sleep rhythms of the electroencephalogram. *J Neurosci* 13(8):3266–3283.